System Identification of a NiTi-Based SMA Actuator

Luiz F. Toledo, Joey Z. Ge, Juan M. Oxoby, Ying Chen, and Néstor O. Pérez-Arancibia

***Abstract*— We present an experimental method for the modeling and system identification of wire actuators made from *shape memory alloys* (SMAs). The proposed approach employs minimum-variance adaptive tuning and control to find parameters for a modified Preisach model that can represent the hysteresis of SMA-based actuators. Thermally- and mechanically-induced phase transformations, known as the *shape memory effect* (SME) and superelasticity (or pseudoelasticity), respectively, allow the recovery of plastic deformation and enable SMA wires to behave as actuators. Both types of phase transformation display hysteretic nonlinearities in the backward and forward directions. Here, we classify the SME phase transformation hysteresis and modify the classical Preisach model to account for experimentally observed superelasticity. The proposed actuator model is validated with experiments in which an SMA wire is statically and dynamically loaded.**

I. Introduction

Presently, the power autonomy of electrically-driven microrobots is prevented by limitations in micro-scale battery technology [1]. This has motivated us to explore new micro power and actuation technologies based on *shape memory alloys* (SMAs) and flameless catalytic combustion. The envisioned actuator technology is motivated by medium- and high-temperature SMAs such as *nickel-titanium* (NiTi), *nickel-titanium-platinum* (NiTiPt) or *nickel-titanium-palladium* (NiTiPd) [2], [3]. Thermally- and mechanically-induced phase transformations known as the *shape memory effect* (SME) and superelasticity (or pseudoelasticity), respectively, allow the recovery of seemingly plastic deformations. These phenomena transform SMAs between austenitic and martensitic phases and display hysteretic behavior. We propose an experimental method to identify the temperature-stress-strain mappings that govern the actuation properties of SMA wires. The suitability of the proposed approach is demonstrated using a medium-temperature NiTi SMA wire.

The thermodynamics of the SMA wire are described by a model derived from first principles. The nonlinear mapping characterizing the actuation properties is described by a proposed modified Preisach model. By controlling the temperature and stress, the nonlinear temperature-stress-strain mapping is identified for the ranges 25-75°C and 50-200 MPa. For these operating conditions, complete characterization of the phase transformation hysteresis allows us to explore the design space of SMA-based actuators and improve their configurations for specific performance objectives such as high-frequency or low-temperature actuation. The method discussed here can also be used to identify other SMA-based actuators such as NiTiPd-based wires which operate at high temperatures.

This extended abstract presents results to be published in the Proceedings of the 2017 *American Control Conference* (ACC-2017). This work was partially supported by the *National Science Foundation* (NSF) through award NRI 1528110 and the USC Viterbi School of Engineering through a start-up fund to N. O. Pérez-Arancibia. Any opinions, findings, conclusions or recommendations expressed in this material are those of the authors and do not necessarily reflect the views of the NSF.

L. F. Toledo, J. Z. Ge, Y. Chen, and N. O. Pérez-Arancibia are with the Department of Aerospace and Mechanical Engineering, University of Southern California (USC), Los Angeles, CA 90089-1453, USA (e-mail: ltoledo@usc.edu, zaoyuang@usc.edu, chen061@usc.edu, and perezara@usc.edu). J. M. Oxoby is with iRobot, Pasadena, CA 91107, USA (e-mail: joxoby@irobot.com).

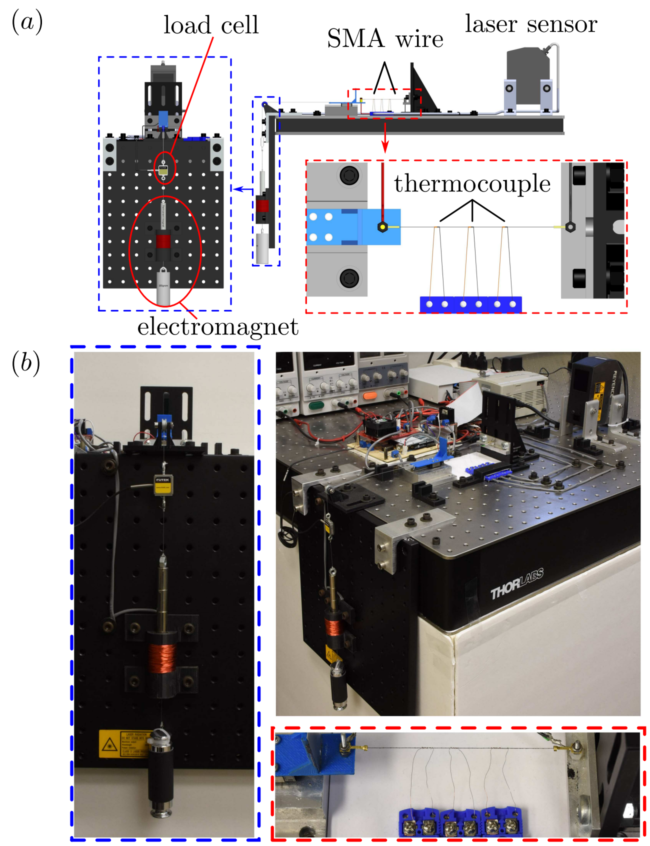

Fig. 1. (a) CAD model and (b) picture of the experimental setup. The SMA wire is electrically heated and the temperature is measured by thermocouples, as highlighted by the red boxes in (a) and (b), and controlled using the adaptive scheme presented in [4]. To allow for proper installation of the thermocouples, an electrically-insulative epoxy is used. The stress is applied, measured, and controlled using an electromagnet, a load cell, and a PID controller, respectively, as highlighted by the blue boxes in (a) and (b). The contraction due to phase transformations is measured by a laser sensor, shown on the right in (a) and (b).

II. Experimental Setup and SMA Actuator Model

The experimental setup is shown in Fig. 1. This configuration was designed to be controllable such that precise values of stress and temperature can be inputted to the wire actuator while accurate measurements of contraction and expansion can be obtained. These experimental data, along with the identification procedure proposed in [4], are used to estimate an operator that maps stress and temperature to strain. In this case, the SMA-based actuator is electrically heated, resulting in a thermodynamic behavior described by first principles as

$$m c_{\mathrm{p}} \dot{T}(t) = R_{\mathrm{w}}(\xi) i^2(t) - hA\left(T(t) - T_\infty\right), \qquad (1)$$

where t is time, c_{p} is the specific heat of NiTi, h is the heat transfer coefficient for convection in air, T_∞ is the ambient temperature, and m, R_{w}, i, A, T and ξ are the mass, resistance, electric current, surface area, temperature and

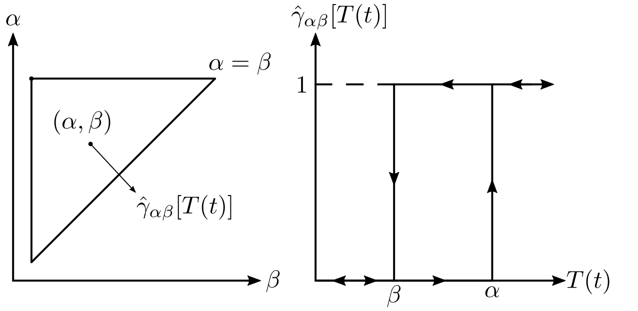

Fig. 2. The hysteron operator on the Preisach plane. The hysteron operator switches *on* at α when $T(t)$ is increasing and *off* at β when $T(t)$ is decreasing.

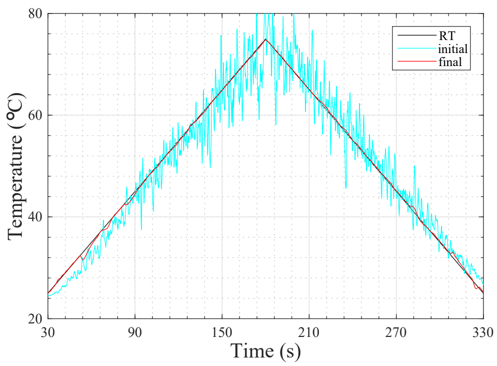

Fig. 3. Temperature tracking performance comparison between the initial setup, composed of a PID controller with one type K thermocouple, and the final setup, consisting of the adaptive controller presented in [4], three type T thermocouples, and electrically-insulating epoxy.

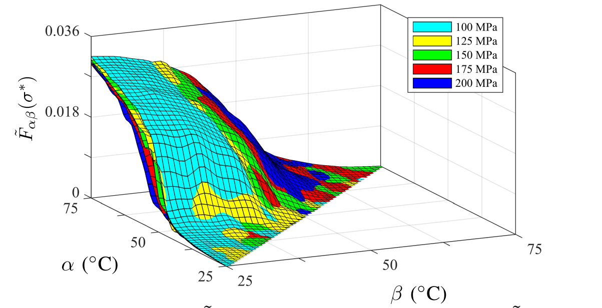

Fig. 4. Set of 3-D *slices* $\tilde{F}_{\alpha\beta}(\sigma)$ of the identified function $\tilde{F}(\alpha, \beta, \sigma)$, for $\sigma^* = 100$, 125, 150, 175 and 200 MPa.

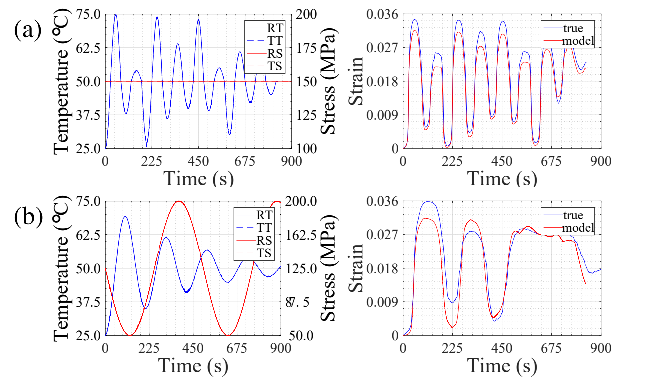

Fig. 5. Results of system validation experiments for (a) statically and (b) dynamically loaded conditions. The input reference temperature (RT) and stress (RS) and the true temperature (TT) and stress (TS) are shown on the left. The resulting strain is shown on the right.

mole fraction of martensite of the SMA wire, respectively. $R_{\text{w}}(\xi)$ is a nonlinear term resulting from the hysteretic properties of SMAs, but in this case is approximated as a constant.

For regions in which phase transformation hystereses occur, the material mechanics can be described by the time-dependent modified Preisach model

$$\epsilon(t) = \iint_{\alpha \geq \beta} \mu(\alpha, \beta, \sigma) \hat{\gamma}_{\alpha\beta}[T(t)] d\alpha d\beta, \qquad (2)$$

where ϵ and σ are the strain and stress of the SMA wire, respectively. The function μ is a *Preisach distribution* (PD) as defined in [4], α and β are coordinates of the Preisach plane, and $\hat{\gamma}_{\alpha\beta}$ are hysteron operators defined for a pair (α, β) on the Preisach plane with argument $T(t)$, as defined in Fig. 2. When the SMA wire is fully austenitic or martensitic, the material mechanics can be linearized as in the classic metallic case. A full description of the modified Preisach model and its implementation can be found in [4].

III. System Identification

To obtain data for system identification, feedback controllers that track stress and temperature were implemented. As described in [4], to achieve the desired measurement accuracy, several control methods were employed in an iterative design process. For example, Fig. 3 shows the control performances attained using a simple *linear time-invariant* (LTI) controller (initial) and a combined adaptive-minimum-variance gain-scheduling controller (final).

The identification of μ requires differentiation of experimental data, which can amplify errors embedded in the data. To avoid this, we identify a distribution of output increments $F(\alpha, \beta, \sigma)$, related to μ as follows. At a constant stress σ^*, the temperature of the SMA wire is increased to α^* then decreased to β^*. The hysterons that turn off during this input reversal process form a triangular region R bounded by the lines $\alpha = \beta$, $\alpha = \alpha^*$, and $\beta = \beta^*$. The resulting incremental change in output for this input reversal process is given by $F(\alpha^*, \beta^*, \sigma^*) = \iint_R \mu(\alpha, \beta, \sigma^*) \, d\alpha d\beta$. In this case, the experimentally identified distribution $\tilde{F}(\alpha, \beta, \sigma)$ cannot be visualized because it defines a 4-D hypersurface. However, we can visualize 3-D *slices* of $\tilde{F}$, $\tilde{F}_{\alpha\beta}(\sigma^*)$, as shown in Fig. 4. The results from the model validation experiments for static and dynamic loading are presented in Fig. 5.

IV. Conclusion

We presented an experimental method for the modeling and system identification of a NiTi-based SMA wire actuator. The accuracy of the identified model was tested experimentally under statically and dynamically loaded conditions. In both cases, the model generally describes the dynamics of the SMA-based actuator. The model accurately predicts transitions between maxima and minima; however, minor discrepancies are observed at the extrema.

References

[1] R. J. Wood, B. Finio, M. Karpelson, K. Ma, N. O. Pérez-Arancibia, P. S. Sreetharan, H. Tanaka, and J. P. Whitney, "Progress on 'pico' air vehicles," *Int. J. Robot. Res.*, vol. 31, no. 11, 2012.

[2] W. Huang, "On the selection of shape memory alloys for actuators," *Mater. & Des.*, vol. 23, pp. 11–19, Feb. 2002.

[3] D. J. Hartl and D. C. Lagoudas, "Aerospace applications of shape memory alloys," *Proc. Inst. Mech. Eng., Part G: J. Aerosp. Eng.*, vol. 221, no. 4, pp. 535–552, Apr. 2007.

[4] L. F. Toledo, J. Z. Ge, J. M. Oxoby, Y. Chen, and N. O. Pérez-Arancibia, "System identification of a NiTi-based SMA actuator using a modified Preisach model and adaptive control," in *Proc. Amer. Control Conf.*, May 2017.